High Resolution AFM Images of the Single-Crystal α-Al_2O_3(0001) Surface in Water

Yang Gan* and George V. Franks

Chemical Engineering, School of Engineering, University of Newcastle, Callaghan, NSW 2308, Australia

Received: March 9, 2005; In Final Form: May 5, 2005

The (0001) surface of α-Al_2O_3 single crystals has been imaged by atomic force microscopy in water. The observed hexagonal lattice arrangement has a period of 4.7 Å, in good agreement with the known bulk unit cell. The sample cleaning procedure was found to be crucial in obtaining clean terraces and achieving lattice resolution.

1. Introduction

Alumina (Al_2O_3) has important applications in catalysis,[1] ceramics processing,[2] and epitaxial growth of films.[3] Natural corundum (α-Al_2O_3) has also been intensively studied for its importance in minerals processing and the adsorption of heavy metal elements.[4,5] In these applications, the surface of alumina plays a key role in controlling adsorption, reaction, and deposition. The bulk structure of corundum has oxygen atoms arranged in approximately hexagonal close-packed layers. Between any two layers of oxygen (O) atoms, only two-thirds of the octahedral sites are filled by aluminum (Al) atoms. The hexagonal unit cell's size is $a = 4.76$ Å, $c = 13$ Å.[6] In aqueous solution or in humid air (where most applications occur), the dominant surface species are surface hydroxyl groups.[7]

In a vacuum, the α-Al_2O_3(0001) surface has been extensively characterized by low energy electron diffraction (LEED)[8] and X-ray diffraction (XRD) methods.[9,10] Both the bulklike (1×1) structure and other high temperature structures such as $(\sqrt{3} \times \sqrt{3})$R30° and the complex $(\sqrt{31} \times \sqrt{31})$R±9° have been observed. Depending on the surface preparation procedures, both Al-terminated and O-terminated surfaces have been found to occur, as illustrated in Figure 1.

In a humid atmosphere or water, partially and fully hydroxylated α-Al_2O_3(0001) surfaces have been characterized by LEED,[8] X-ray methods,[9,10] and dynamic-mode scanning force microscopy (SFM).[11] Using a dynamic scanning force microscopy technique, Barth and Reichling investigated a reconstructured surface.[11] They imaged a $(\sqrt{31} \times \sqrt{31})$R±9° structure produced at 1300 °C in ultrahigh vacuum with atomic resolution. After exposure to millipascal or lower levels of water vapor, they observed many clusters of the size 0.4−0.8 nm. They supposed these clusters were most probably crystalline $Al(OH)_3$. As early as 1993, Steinberg et al.[12] successfully achieved unit cell resolution images of nanocrystalline α-Al_2O_3 that was grown on mica by the van der Waals epitaxy method. The 10 nm thick alumina films were grown on freshly cleaved mica sheets by vacuum depositing from a pellet vaporized using an electron beam. They observed a hexagonal lattice (period of 4.7 ± 0.2 Å) at various places on the film in both force and height modes in air, water, and salt solutions that was claimed to be reproducible over a period of weeks.

Calculations based on first principles indicate that, in the presence of water vapor, strong surface relaxation occurs due to interaction between water molecules and the surface.[13−15] When exposed to water vapor, the unhydrated Al-terminated surface reacts to form a hydroxyl group (OH)-terminated surface (the coverage of −OH depends on the coverage of water molecules). Fully hydroxylated surfaces with more than one layer of water molecules have been found to be gibbsite-like, that is, a surface $Al(OH)_3$ phase. This viewpoint has also gained support from IR spectra studies on water adsorption on α-Al_2O_3(0001) surfaces.[16]

Several studies have also focused on the measurement of surface forces arising from α-Al_2O_3.[2,17,18] Up to now, atomic resolution of the α-Al_2O_3(0001) surface of single-crystal bulk samples in water has not been achieved by atomic force mircroscopy (AFM). The first difficulty is to get high quality single crystals. It can be found[19] that raw alumina single crystals polished by the manufacturer showed great differences: some have clearly visible surface steps as-received, while others need further treatments. The other concern is surface contamination. In high vacuum environments, it is relatively easy to clean the surface by high temperature annealing and ion bombardment after simple chemical pre-etching treatments. However, under ambient atmospheric conditions, it is more difficult to get a clean enough surface for stable high resolution AFM imaging. A good indication of a clean single-crystal surface is that surface steps can be observed on a single-crystal sample. Thus, the first step to successful atomic scale imaging of the α-Al_2O_3(0001) surface should be to achieve a clean and step-revealing surface.

In this paper, we show that the atomic scale features of the α-Al_2O_3(0001) surface can be imaged by contact-mode AFM in water after careful surface cleaning. Possible surface structures and imaging mechanisms are discussed in order to explain the observed periodicity of regular surface corrugations.

2. Experimental Procedures

2.1. Materials. α-Al_2O_3 single crystals with (0001) orientation were purchased from MTI, Richmond, CA (note that these samples were produced in about 1998). The specifications given by the manufacturer are the following: crystal purity, 99.99%; orientation tolerance, ±0.5°; surface roughness, <10 Å; surface flatness, <2 μm/cm. The size of the crystals is 10 mm × 10 mm × 0.5 mm. The water used was Milli-Q deionized (DI) (resistivity 18.2 MΩ·cm) and filtered with a 0.2 μm filter. AR grade ethanol was once distilled before use.

2.2. Cleaning Procedures. Because the samples had been stored for several years, the surfaces were quite dirty. The same

* Corresponding author. Fax: 61 2 49216920. E-mail: yang.gan@newcastle.edu.au.

10.1021/jp0512053 CCC: $30.25
Published on Web 06/04/2005

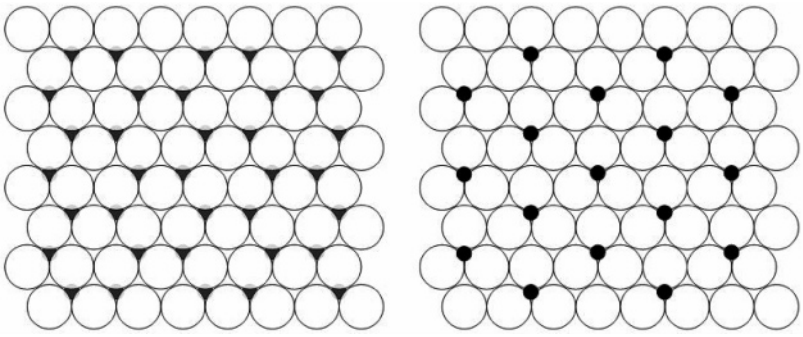

Figure 1. Schematics of two types of surface termination of the α-Al_2O_3(0001) surface in a vacuum: (left) (1 × 1) O termination; (right) ($\sqrt{3}\times\sqrt{3}$) single Al termination. Large open circle, O atom; small solid circle, Al atom.

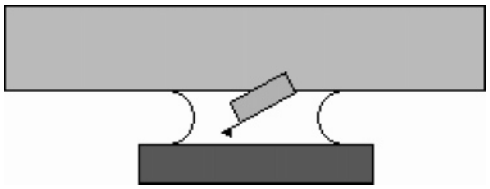

Figure 2. Sample and probe setup. A small volume of water was directly injected between the AFM solution cell and the sample. No O-ring was used.

cleaning procedure as that used by Franks and Meagher[18] was tried as well as the following modified procedure: immersed in surfactant solution (1% Decon surfactant, 20% ethanol, 79% DI water) for 48 h; DI water rinse (10 times); ethanol, sonicated for 20 min; DI water rinse (3 times); DI water, sonicated for 20 min; UV light exposure for 30 min; H_2SO_4 + H_2O_2 (4:1 volume ratio, called piranha in microelectronics industry) for 20 min (this solution was used by Kershner et al.[20] for cleaning α-Al_2O_3 single-crystal samples); finally, the crystals were fully rinsed with DI water.

Both cleaning procedures were found to be effective, and similar images were found for both procedures. The modified procedure was believed to be slightly superior and was used for all results in this paper.

2.3. Atomic Force Microscopy. A Nanoscope III atomic force microscope (Digital Instruments Inc., Santa Barbara, CA) was used. The E scanner was used with a maximum scanning size of 10 μm × 10 μm. Silicon nitride probes were used; the nominal tip radius ranges from 20 to 60 nm. The probes were also soaked in piranha solution for 20 min and then fully rinsed with DI water. The cantilever's spring constant varies from 0.06 to 0.58 N/m (nominal value) depending upon the choice of the four cantilevers available. While in atomic scale imaging, only the softest cantilevers with a spring constant of 0.06 N/m were used. During scanning, the set point was adjusted to keep the tip−sample force in the range of nanonewtons.

Because it has been found that the O-ring used in the fluid cell caused serious distortion of atomic scale images, all images have thus been captured without using an O-ring. DI water was injected slowly between the fluid cell and sample to ensure that wetting propagated slowly along the probe and no air bubbles were left on the reflecting coating of the cantilever. A meniscus of water formed between the sample and the lower surface of the fluid cell. The setup is illustrated in Figure 2. To maintain at least 2 h of AFM imaging without refilling, a large portion of the sample's surface was covered with water.

The sample was glued to a magnetic sample pack using double-sided adhesive tape (3M, Minnesota). Clean stainless steel tweezers were used to press the sample's edges against the sample pack so that a strong adhesion was formed (no large air bubble was trapped between the surface and the tape). All AFM measurements were conducted at room temperature (25 ± 2 °C). Before engagement, the whole system was turned on and left to be stabilized for at least 1 h.

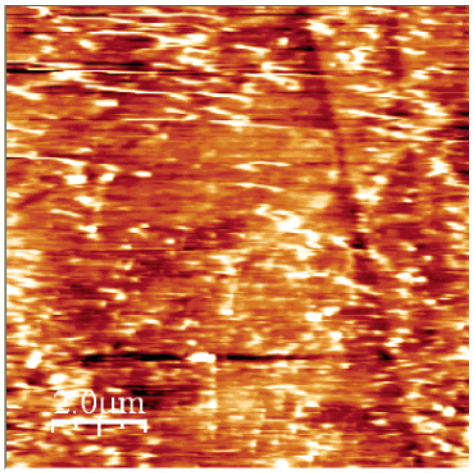

Figure 3. α-Al_2O_3(0001) surface imaged in air, only rinsed with ethanol (image size 10 μm × 10 μm).

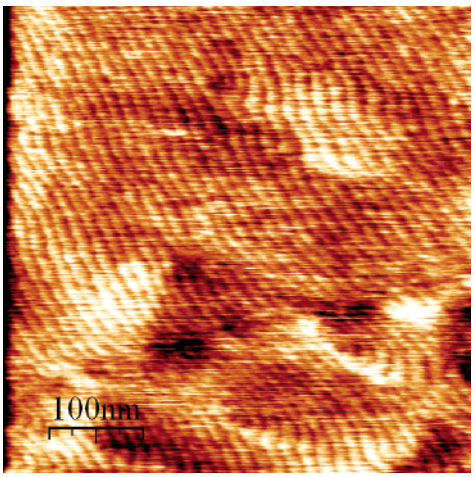

Figure 4. Surface terraces are revealed after cleaning. Most terraces are parallel. Some irregularities are believed to be caused by polishing and sonicating treatments (image size 400 nm × 400 nm).

3. Experimental Results

Initially, as-received samples were rinsed only with ethanol three times to remove large particles and then dried with high velocity pure nitrogen gas. Figure 3 is a 10 μm × 10 μm AFM image taken in air. The surface appears very dirty. Several large polishing scratches are visible on the surface. Besides some

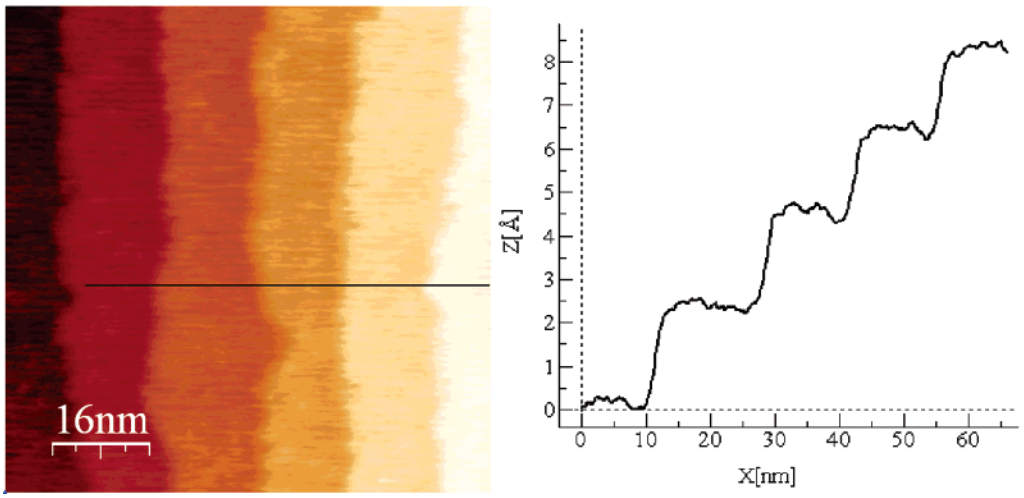

Figure 5. Several nearly parallel steps on the α-Al_2O_3(0001) surface: (left) Each band of color corresponds to a flat planar step. Each step is about 15 nm wide. (right) Line profile along the black line (in the left panel) across five steps. The step height is about 2 Å (image size 80 nm × 80 nm).

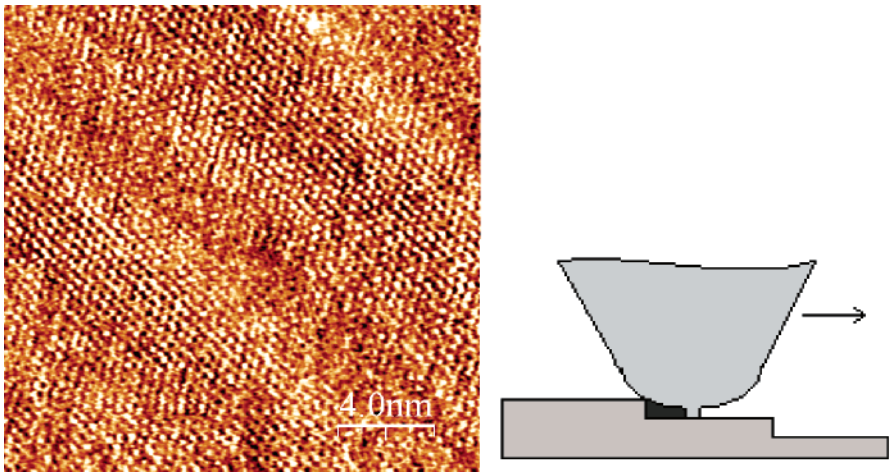

Figure 6. (left) Periodic corrugations can only be resolved in diagonal regions from the upper left to lower right corner (deflection image, size 20 nm × 20 nm). (right) An illustration of why regions adjacent to a step edge on the surface cannot be imaged by a real tip.

particles, horizontal artifacts in the image are believed to be caused by organic contaminants which cause strong tip−surface adhesion.

After cleaning, many terraces were found across the surface. Figure 4 is a 500 nm × 500 nm image taken in water. (All of the following images presented in this paper are taken in water.) On this scale, not all steps appear straight and parallel, which is believed to be caused by polishing and sonicating treatments. However, at a smaller scale, parallel and straight steps can be found (Figure 5, left). The mean step width is 15 nm; the height of single steps has been determined to be about 2 Å by a profile analysis (Figure 5, right). This value is very close to the 2.1 Å distance between two adjacent O-planes.[21,22] It should be noted that no multiheight steps have been found across the surface; this is quite contrary to very high temperature annealed samples.[23]

At the nanoscale, there is an important point to be noticed in our images. As shown in Figure 6, left, between two stripes showing regular lattice points parallel to the step, there are regions about 4 nm wide where lattice points cannot be resolved. There is only a diagonal stripe 4−5 nm wide where clearly visible lattice points can be resolved. This can be attributed to the finite sharpness of the tip. Simple geometry shows that a tip radius of 40 nm is unable to probe a width of 4.1 nm adjacent to a 2.1 Å high step. A tip can be visualized as in Figure 6, right. A small apex, which may consist of many atoms, protrudes from the blunt end of the tip. When the tip is scanning over a step, the apex cannot access the region of the terrace near the step. In the inaccessible area, the side of the tip may scan against the step edge, resulting in noise on the image. After that, this apex resumes good resolution.

On the atomic scale, periodic corrugations can be clearly resolved. Two images in deflection mode of the same area are shown in parts a and b of Figure 7 in which the tip raster scans from upside to downside and reversely, respectively. The two images are nearly identical. This indicates that the atomic force microscope was well calibrated and stabilized so that no apparent drift persisted. If not, usually two images look quite different due to drift.[24] Both images show hexagonal periodic corrugations. Figure 7c is the corresponding two-dimensional fast fourier transformation (2d-FFT) pattern of Figure 7a. The period of hexagonal lattice arrangements can be determined as 4.7 ± 0.4 Å.

For a better visualization of the periodic arrangements, a "doughnut type" 2d-FFT filtering treatment[25] is conducted in Figure 7a. This is different from the common 2d-FFT procedure. The procedure used to produce Figure 8 selects only data from a doughnut shaped region that contains most of the information for the hexagonal lattice for transformation. In this way, a realistic surface lattice arrangement can be obtained.

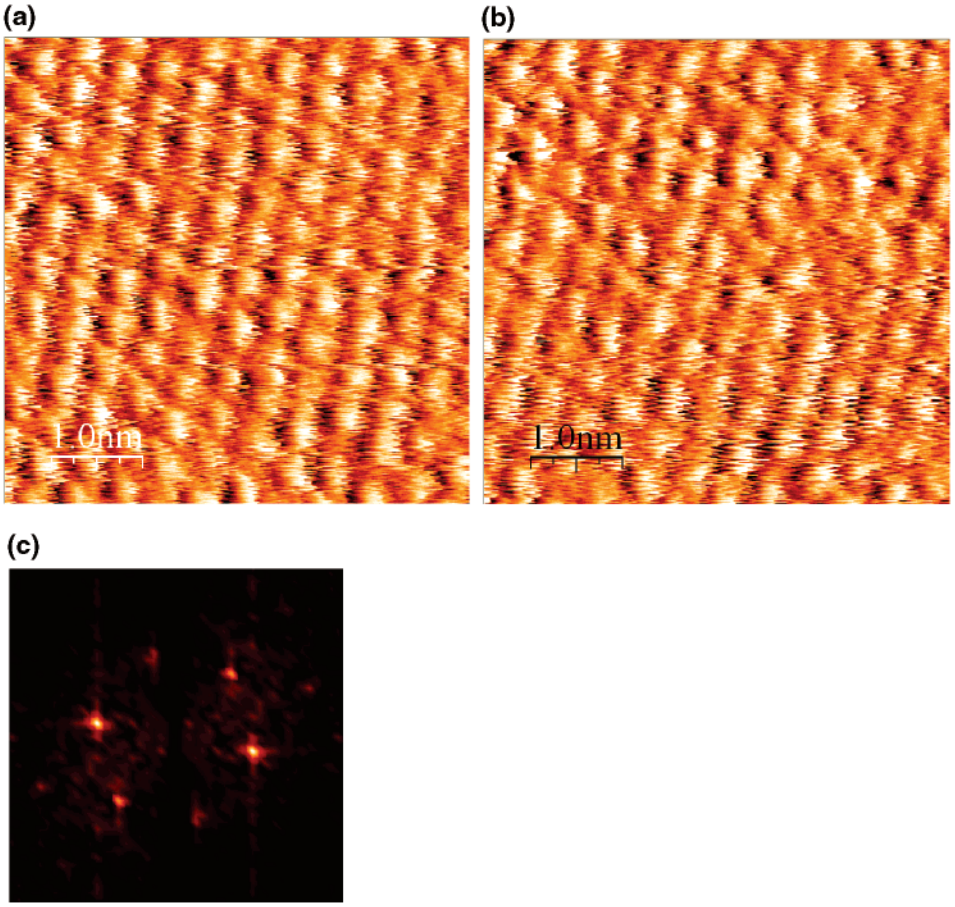

Figure 7. Regular corrugations resolved on two continuously captured images with opposite slow scanning direction: (a) the AFM tip moves from upside to downside scanning; (b) the tip moves from downside to upside scanning (deflection image, size 5 nm × 5 nm); (c) the 2d-FFT pattern of part a. The period was determined to be 4.7 ± 0.4 Å.

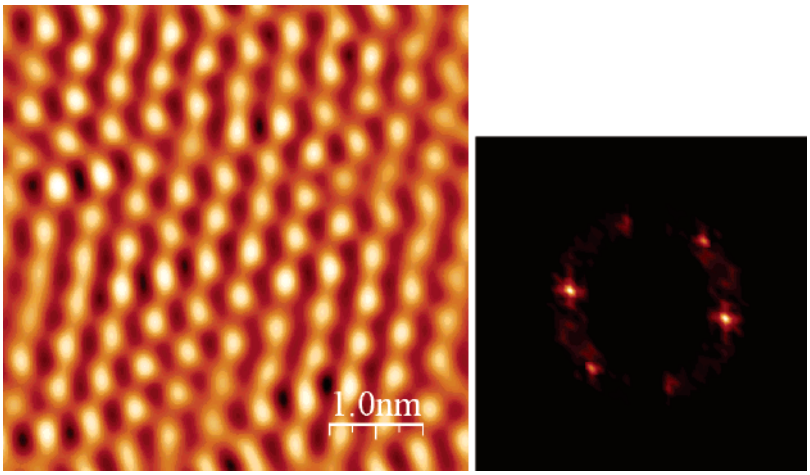

Figure 8. (left) 2d-FFT transformed image from Figure 7a. (right) The corresponding truncated doughnut type 2d-FFT pattern. In this transformation, only periodic components (in a doughnut shape) close to the bright points were selected for transformation.

4. Discussion

4.1. Cleaning Procedure. A proper cleaning procedure is crucial to get clean surfaces and achieve atomic resolution. During this study, several different cleaning methods have been used to check if they are effective in cleaning samples (results not shown in the paper). It was found that it was not easy to get the samples completely free of contaminants before AFM imaging; organic contamination and dust from the air or container are strongly adhered to the surface (Figure 3). Although no XPS tests were performed to check if there were any organic contaminants on the surface, after cleaning large areas of terraces remain resolvable by AFM for at least 2 h in water (see Figures 4 and 5). This indicates that our samples' surfaces and water used are very clean. It was found that the tip occasionally got contaminated during scanning. Sometimes bad images persisted for a short time, but after repeat scanning and varying the setpoint (i.e., interaction force), usually high resolution would resume.

4.2. Atomic Arrangements of the α-Al_2O_3(0001) Surface. In Figure 9, two sets of hexagonal lattices with a period of 4.7

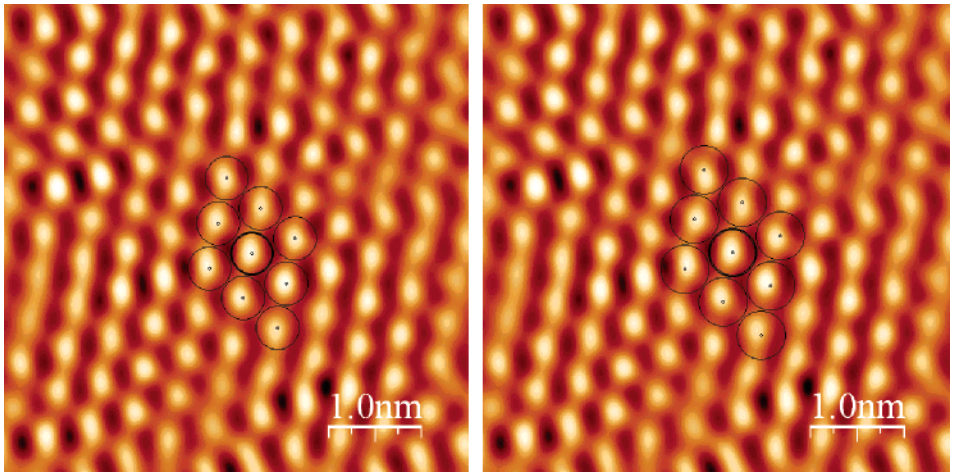

Figure 9. Hexagonal lattice arrangements of two lattice sizes were imposed onto the left image of Figure 8: (left) 4.7 Å of this study; (right) 5.2 Å of mica's.

and 5.2 Å (mica's lattice constant), respectively, are superimposed onto the captured image (Figure 8). It is clear that the first hexagonal lattice coincides well with the AFM image, while mica's does not. We also imaged mica and found good agreement between the mica images and the 5.2 Å lattice. Because the difference of lattice period of α-Al_2O_3 and mica is quite small (0.5 Å), the ability of AFM in clearly determining this difference proves that the atomic force microscope is a very powerful tool in surface structure studies of oxides. The lattice period of the bulk sample found in this study is in good agreement with that of the thin film sample of Steinberg's (4.7 ± 0.2 Å) and the bulk unit cell size (4.76 Å).

If the surface were terminated in oxygen, as shown in Figure 1, left, as supported by diffraction[10] and first-principles simulations,[13−15] these O atoms would react to form hydroxyl (OH) groups when exposed to water; then, the distance between nearest OH groups will be equal to the O−O distance: 2.74 Å. Since $\sqrt{3} \times 2.74 = 4.75$ Å, we may refer to the observed structure (hexagonal periodicity of 4.7 Å) as a $\sqrt{3} \times \sqrt{3}$ structure.

However, the question remains of why the α-Al_2O_3(0001) surface shows a 4.7 Å hexagonal lattice arrangement because one would expect AFM images of hexagonal arranged OH groups with a periodity of 2.74 Å. We have failed to observe any 2.74 Å periodic structures with our sample after trying many tips, varying scanning directions, and minimizing the tip−surface force. This fact may be accounted for by considering the resolution of AFM and the actual surface structure.

First, we may only have obtained unit cell scale resolution but not true atomic resolution. We have not yet been able to image single atoms or OH groups. There is debate in the scientific community concerning the ability to measure true atomic resolution with AFM.[26−28] It is not very clear why lattice resolution of surfaces (especially layered solids such as mica and graphite) can be achieved by contact-mode AFM even though a tip's radius is at the scale of tens of nanometers. It involves complex interactions during sliding contact between a tip and solid surface. There have been several models proposed to address this issue. Conversely, several authors have shown that true atomic scale images may be obtained under the proper operating conditions.[29−31]

The lateral resolution of AFM is mainly limited by the probe's tip radius and liquid composition (these two factors control the force between the tip and the sample). The van der Waals (VdW) force between the tip and the surface is in direct proportion to the tip radius. To achieve true atomic resolution, in principle, there should be only one atom on the very end of the tip contributing to the topological signal, and the maximum force for true atomic resolution will be less than 10^{-11} N (10 pN).[29] However, the common AFM contact-mode silicon nitride probes have a tip radius of usually 20−40 nm, so the VdW force is on the scale of nanonewtons. This force is still too high to ensure true atomic resolution. Even if occasionally a fresh 20 nm tip is atomically sharp at the very end during the engaging process, the large VdW force will cause a sudden jump-in of the tip, causing crushing of the apex and loss of sharpness. Therefore, to achieve true atomic resolution of the α-Al_2O_3(0001) surface, atomically sharp tips with a high aspect ratio should be used.

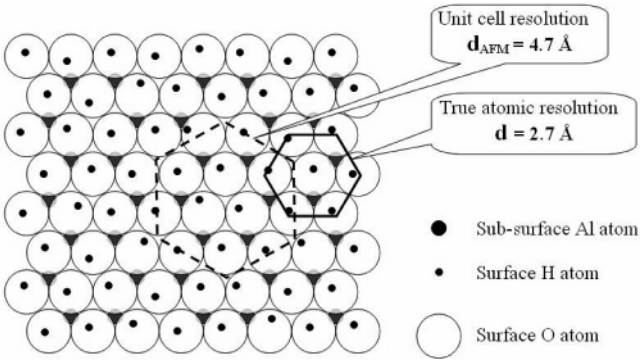

Figure 10. Illustration showing that the single surface hydroxyl group may not be resolved with atomic resolution; instead, only octahedral vacant sites were imaged with unit cell resolution. An ab initio simulation study[13−15] suggested that hydrogen bonds between neighboring OH groups tend to cause some OH groups to lie down toward octahedral vacant sites.

The other possibility is that the orientation difference of surface hydroxyl (OH) groups on an oxygen-terminated α-Al_2O_3(0001) surface may result in a hexagonal 4.7 Å arrangement. On the completely hydroxylated α-Al_2O_3(0001) surface, there are three OH groups bound to (and above) each Al atom (see Figure 10). Simulation studies[13−15] showed that at any particular instant two of those OH groups are nearly vertical to the surface, while the remaining one is lying flat on the surface in a position just above the unoccupied octahedral site just below. This occurs because of hydrogen bonding between adjacent OH groups over the hollow space above the unoccupied octahedral sits. The unoccupied octahedral sites have a hexagonal structure with a periodicity of about 4.76 Å in bulk α-Al_2O_3. If it is assumed that the tip could not resolve these

three OH groups, instead only the center of those three OH groups could be resolved, the AFM image would show the same lattice arrangement as the Al-terminated surface: a unit cell size of 4.70 Å. Simulations can be used to address this issue.

The other less likely possibility is that the surface is ($\sqrt{3} \times \sqrt{3}$) single Al-terminated (like Figure 1, right). Then, the images could be explained by assuming that the high points are due to Al−OH groups with a period of about 4.7 Å. We believe this scenario is not likely due to the abundance of evidence[10,13−15,32] that indicates the hydroxylated surface is terminated with densely packed OH groups.

Further studies from both experimental and simulation points of view are definitely required to understand the AFM imaging mechanism of the alumina surface.

5. Conclusions

The α-Al_2O_3(0001) surface in water has been imaged by AFM. In the vertical direction, steps with 2.1 Å height are observed corresponding to the thickness of a single closely packed oxygen layer. In the lateral direction, lattice scale images are resolved. A hexagonal lattice arrangement has been found with a periodicity of 4.7 Å which is consistent with the periodicity of the unoccupied octahedral sites between the topmost and underlying oxygen layers. The appropriate surface cleaning procedure is found to be crucial to observing these features.

Acknowledgment. The authors would like to acknowledge support form the Australian Research Council for Discovery Grant DP0343326. Y.G. would like to thank the University of Newcastle for support through the University of Newcastle Research Fellow Scheme. Thanks to Dr. Erica Wanless for the use of the AFM facility and stimulating discussions.

References and Notes

(1) Knözinger, H.; Ratnasamy, P. *Catal. Rev. Sci. Eng.* **1978**, *17*, 31.
(2) Ducker, W. A.; Xu, Z.; Clarke, D. R.; Israelachvili, J. N. *J. Am. Ceram. Soc.* **1994**, *77*, 437.
(3) Heinrich, V. E.; Cox, P. A. *The Surface Science of Metal Oxides*; Cambridge University Press: Cambridge, U.K., 1994.
(4) Brown, G. E., Jr.; Henrich, V. E.; Casey, W. H.; Clark, D. L.; Eggleston, C.; Felmy, A.; Goodman, D. W.; Grätzel, M.; Maciel, G.; McCarthy, M. I.; Nealson, K. H.; Sverjensky, D. A.; Toney, M. F.; Zachara, J. M. *Chem. Rev.* **1999**, *99*, 77 and references therein.
(5) Bargar, J. R.; Towle, S. N.; Brown, G. E., Jr.; Parks, G. A. *J. Colloid Interface Sci.* **1997**, *185*, 473.
(6) Bragg, L.; Claringbull, G. F. *Crystal Structures of Minerals*; G. Bell and Sons Ltd.: London, 1965.
(7) James, R. O. Characterization of Colloids in Aqueous Systems. In *Ceramic Powder Science*; Messing, G. L., Mazdiyasni, K. S., McCauley, J. W., Haber, R. A., Eds.; Advances in Ceramics; American Ceramic Society: Westerville, OH, 1987; Vol. 21.
(8) Soares, E. A.; Van Hove, M. A.; Walters, C. F.; Mccarty, K. F. *Phys. Rev. B* **2002**, *65*, 195405 and references therein.
(9) Liu, P.; Kendelewicz, T.; Brown, G. E., Jr.; Nelson, E. J.; Chambers, S. A. *Surf. Sci.* **1998**, *417*, 53.
(10) Eng, P. J.; Trainor, T. P.; Brown, G. E., Jr.; Waychunas, G. A.; Newville, M.; Sutton, S. R.; Rivers, M. L. *Science* **2000**, *288*, 1029.
(11) Barth, C.; Reichling, M. *Nature* **2001**, *414*, 54.
(12) Steinberg, S.; Ducker, W.; Vigil, G.; Hyukjin, C.; Frank, C.; Tseng, M. Z.; Clarke, D. R.; Israelachvili, J. N. *Science* **1993**, *260*, 656.
(13) Hass, K. C.; Schneider, W. F.; Curioni, A.; Andreoni, W. *Science* **1998**, *282*, 265.
(14) Hass, K. C.; Schneider, W. F.; Curioni, A.; Andreoni, W. *J. Phys. Chem. B* **2000**, *104*, 5527.
(15) Lodziana, Z.; Norskov, J. K.; Stolze, P. *J. Chem. Phys.* **2003**, *118*, 11179.
(16) Al-Abadleh, H. A.; Grassian, V. H. *Langmuir* **2003**, *19*, 341.
(17) Horn, R. G.; Clarke, D. R.; Clarkson, M. T. *J. Mater. Res.* **1988**, *3*, 437.
(18) Franks, G. V.; Meagher, L. *Colloids Surf., A* **2003**, *214*, 99.
(19) Florescu, D. I.; Ramer, J. C.; Armour, E. A.; Thompson, M. Using Atomic Force Microscopy to Control and Enhance Structural and Optical Properties of GaN-based light Emitting Diodes Grown by MOCVD. *Veeco application notes*: http://www.veeco.com/appnotes/AN80_AFM%20MOCVDComp.pdf, 2004.
(20) Kershner, R. J.; Bullard, J. W.; Cima, M. J. *Langmuir* **2004**, *20*, 4101.
(21) Kurnosikov, O.; Pham Van, L.; Cousty, J. *Surf. Sci.* **2000**, *459*, 256.
(22) Yoshida, K.; Yoshimoto, M.; Sasaki, K.; Ohnishi, T.; Ushiki, T.; Hitomi, J.; Yamamoto, S.; Sigeno, M. *Biophys. J.* **1998**, *74*, 1654.
(23) Van, L. P.; Cousty, J.; Lubin, C. *Surf. Sci.* **2004**, *549*, 157.
(24) Henriksen, K.; Stipp, S. L. S. *Am. Mineral.* **2002**, *87*, 5.
(25) Baba, M.; Katitani, S.; Ishii, H.; Okuno, T. *Chem. Phys.* **1997**, *221*, 23.
(26) Burnham, N. A.; Colton, R. J. In *Scanning Tunneling Microscopy and Spectroscopy*: *theory*, *techniques*, *and applications*; Bonnell, D. A., Ed.; VCH Publishers: New York, 1993; p 240.
(27) Hofer, W. A.; Foster, A. S.; Shluger, A. L. *Rev. Mod. Phys.* **2003**, *75*, 1287.
(28) Sokolov, I. Yu.; Henderson, G. S. *Surf. Sci.* **2002**, *499*, 135.
(29) Ohnesorge, F.; Binnig, G. *Science* **1993**, *260*, 1451.
(30) Schimmel, Th.; Koch, Th.; Küppers, J.; Lux-Steiner, M. *Appl. Phys. A* **1999**, *68*, 399.
(31) Sokolov, I. Yu.; Henderson, G. S.; Wicks, F. G. *J. Appl. Phys.* **1999**, *86*, 5537.
(32) Elam, J. W.; Nelson, C. E.; Cameron, M. A.; Tolbert, M. A.; George, S. M. *J. Phys. Chem. B* **1998**, *102*, 7008.